

Analyzing Brightness of Europa's Auroral Footprint with the HST/STIS Dataset Taken in 2014 and 2022

Shinnosuke Satoh¹, Fuminori Tsuchiya¹, Shotaro Sakai¹, Yasumasa Kasaba¹,
Jonathan Nichols², Rikuto Yasuda¹, Tomoki Kimura³

1. Tohoku University, Japan 2. University of Leicester, the UK 3. Tokyo University of Science, Japan



- A1. Transhemispheric electron beam (TEB)
- A2. Europa's oxygen atmosphere
- A3. Space Telescope Imaging Spectrograph
- A4. HST/STIS data analysis: the lead angle
- A5. HST/STIS data analysis: the brightness
- A6. Magnetic field model
- A7. Evaluation of the fitting

A1. Transhemispheric electron beam (TEB)

- Un-reflected Alfvén wave accelerates electrons in Jupiter's ionosphere.
 - Electrons accelerated planetward:
 - Precipitate to Jupiter's upper atmosphere and
 - Excite hydrogen auroras (MAW footprint).
 - Those accelerated **anti-planetward**:
 - travel along the field line and
 - Excite auroras in the other hemisphere.
- Transhemispheric electron beam (TEB) spot

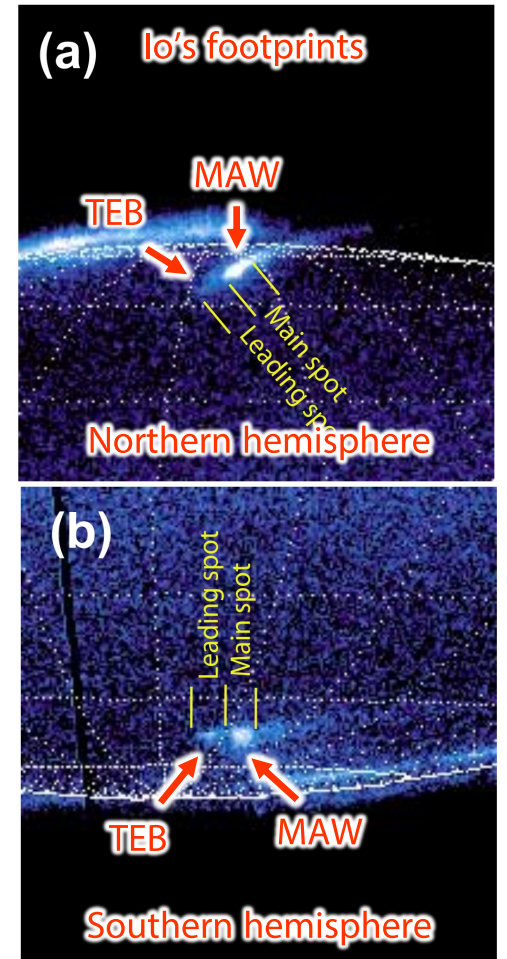


Fig A0101. Io's MAW and TEB spots in both the (a) northern and (b) southern hemispheres taken by the HST/STIS (Bonfond+2008).

A2. Europa's oxygen atmosphere

- A tenuous oxygen atmosphere is generated through radiolysis and sputtering of the water surface.
- Radiolysis of H_2O in the ice by energetic H^+ and O^+ from the magnetosphere.
→ H , H_2 , and O_2
- H , H_2 , and O_2 are sputtered:
 - H and H_2 easily escape.
 - O_2 remains and forms atmosphere.

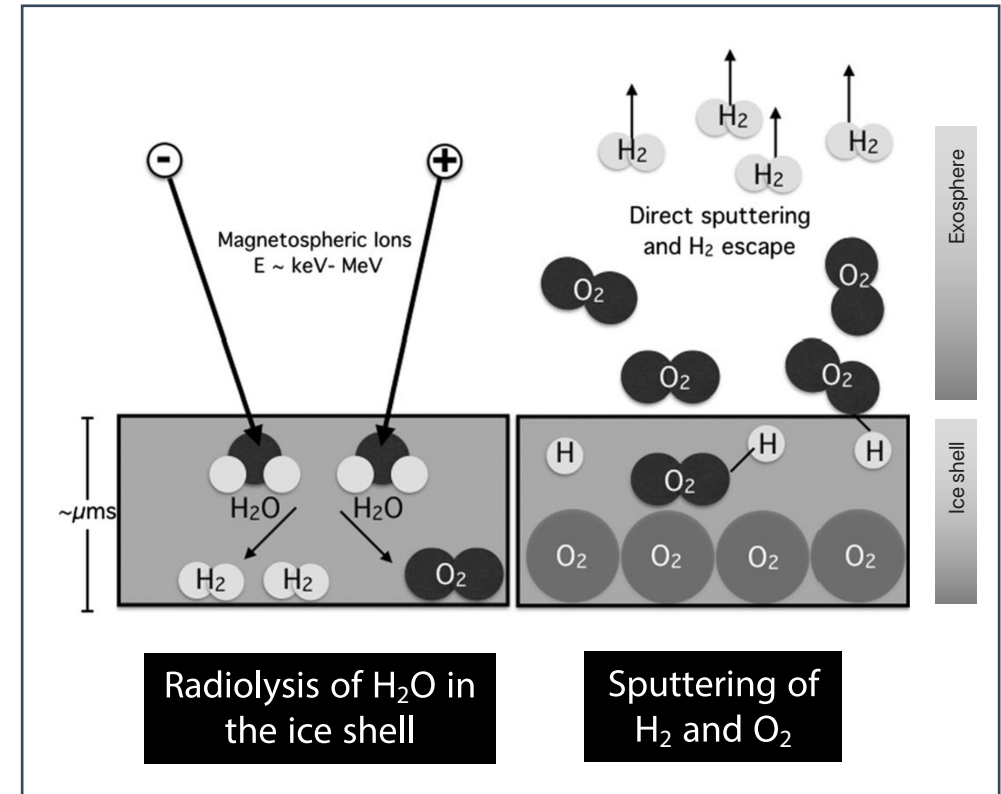


Fig A0201. Creation of the atmospheric neutrals by radiolysis and sputtering on the ice surface (Johnson+2019, modified).

A2. Europa's oxygen atmosphere

- Consists mainly of oxygen molecules mixed with oxygen atoms.
- Sublimated H₂O molecules are also detected around the sub-solar point.
- O₂ column density has been inferred by several HST observations:

Table A0201. Summary of observations by the HST to investigate Europa's atmosphere.

	Hall+1998	Roth+2016	Roth+2021
Instrument	HST/GHRS	HST/STIS	HST/STIS
Year of observations	1994–1996	1999, 2012, 2014–2015	2015
O ₂ column density [cm ⁻²]	(2.4–14) × 10 ¹⁴	(3–6) × 10 ¹⁴	2.47 × 10 ¹⁴ (center) 2.53 × 10 ¹⁴ (limb)
O mixing ratio	< 2% (trailing) < 1.5% (leading)	~ 5% (trailing) ≤ 1% (leading)	-
H ₂ O column density [cm ⁻²]	-	-	2.95 × 10 ¹⁵ (center) < 1 × 10 ¹³ (limb)

A3. Space Telescope Imaging Spectrograph

- The data were acquired by the Space Telescope Imaging Spectrograph on board the Hubble Space Telescope.
- The observations were conducted using the FUV-MAMA (Multi-Anode Microchannel Array) detector with the F25SRF2 filter.

Table A0301. Information of the HST/STIS observations we used in this study.

Proposal ID	13035	16675
Date	January 2014	May–December 2022
Filter	F25SRF2 (130–180 nm)	
Integration	30 seconds	

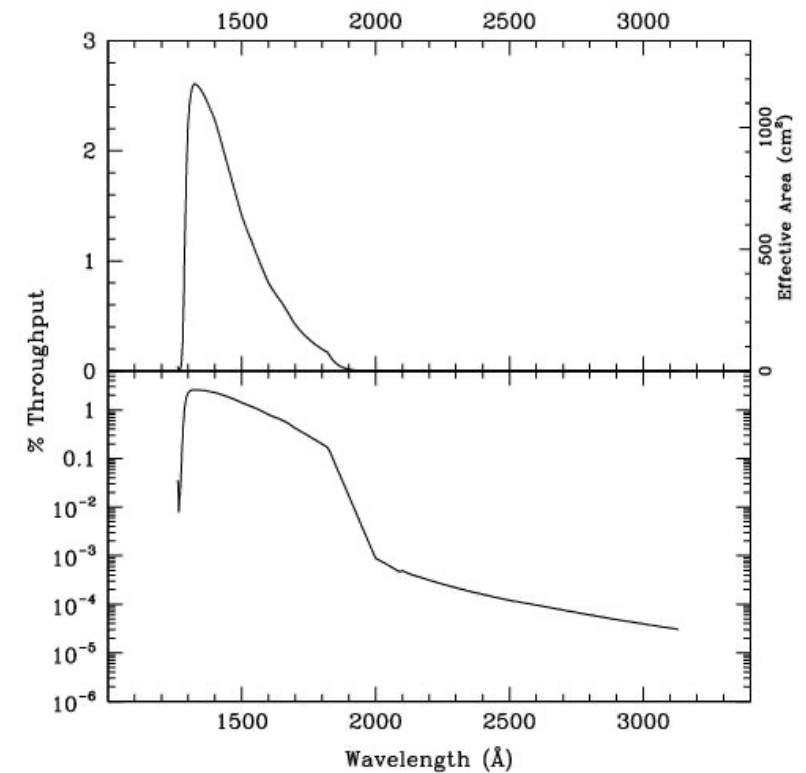


Fig A0301. Throughput of the F25SRF2 filter with the FUV-MAMA detector on HST/STIS (STIS instrument handbook).

A3. Space Telescope Imaging Spectrograph

Data names of the proposal ID 13035 are listed in the following Table Axxx:

sci_data_set_name	sci_targname	sci_start_time	sci_stop_time	sci_actual_duration	sci_pi_last_name
OC1Z01LOQ	JUPITER-NORTH-1	2014-01-01T03:02:53.937000	2014-01-01T03:14:33.937000	700.199875	BADMAN
OC1Z01LUQ	JUPITER-NORTH-1	2014-01-01T03:32:45.937000	2014-01-01T03:45:01.937000	736.19975	BADMAN
OC1Z02TWQ	JUPITER-NORTH-2	2014-01-02T09:19:53.937000	2014-01-02T09:31:33.937000	700.19975	BADMAN
OC1Z02U2Q	JUPITER-NORTH-2	2014-01-02T09:49:45.937000	2014-01-02T10:02:01.937000	736.2	BADMAN
OC1Z05HAQ	JUPITER-NORTH-5	2014-01-05T05:52:00.943000	2014-01-05T06:03:40.943000	700.199875	BADMAN
OC1Z05HGQ	JUPITER-NORTH-5	2014-01-05T06:21:52.943000	2014-01-05T06:34:08.943000	736.19975	BADMAN
● OC1Z06AYQ	JUPITER-NORTH-6	2014-01-06T02:35:18.960000	2014-01-06T02:46:58.960000	700.19975	BADMAN
● OC1Z06B4Q	JUPITER-NORTH-6	2014-01-06T03:05:10.960000	2014-01-06T03:17:26.960000	736.2	BADMAN
OC1Z11LFQ	JUPITER-NORTH-11	2014-01-11T19:39:29.937000	2014-01-11T19:51:09.937000	700.199875	BADMAN
OC1Z11LLQ	JUPITER-NORTH-11	2014-01-11T20:09:21.937000	2014-01-11T20:21:37.937000	736.199875	BADMAN
● OC1Z13B4Q	JUPITER-NORTH-13	2014-01-13T01:56:15.953000	2014-01-13T02:07:55.953000	700.199875	BADMAN
● OC1Z13BAQ	JUPITER-NORTH-13	2014-01-13T02:26:07.953000	2014-01-13T02:38:23.953000	736.199875	BADMAN
● OC1Z12MJQ	JUPITER-NORTH-12	2014-01-16T00:03:33.937000	2014-01-16T00:15:13.937000	700.19975	BADMAN
● OC1Z12MQQ	JUPITER-NORTH-12	2014-01-16T00:33:25.937000	2014-01-16T00:45:41.937000	736.19975	BADMAN

● Data in which the Europa footprint was detected.

A3. Space Telescope Imaging Spectrograph

Data names of the proposal ID 16675 are listed in the following Table Axxx:

sci_data_set_name	sci_targname	sci_start_time	sci_stop_time	sci_actual_duration	sci_pi_last_name
OEOW03CDQ	JUPITER-AURORA-JUNOEM-3	2022-05-20T15:38:53.047000	2022-05-20T16:20:56.047000	2523.19975	NICHOLS
● OEOW09DSQ	JUPITER-AURORA-JUNOEM-9	2022-07-04T18:25:14.237000	2022-07-04T19:07:17.237000	2523.199875	NICHOLS
OEOW10EFQ	JUPITER-AURORA-JUNOEM-10	2022-07-04T21:36:20.220000	2022-07-04T22:18:23.220000	2523.199875	NICHOLS
OEOW11IAQ	JUPITER-AURORA-JUNOEM-11	2022-07-05T13:28:19.227000	2022-07-05T14:10:22.227000	2517.87125	NICHOLS
OEOW13L7Q	JUPITER-AURORA-JUNOEM-13	2022-08-16T22:59:52.297000	2022-08-16T23:07:55.977000	483.549375	NICHOLS
OEOW14P7Q	JUPITER-AURORA-JUNOEM-14	2022-08-17T14:52:21.287000	2022-08-17T14:56:56.967000	275.549375	NICHOLS
● OEOW18QGQ	JUPITER-AURORA-JUNOEM-18	2022-09-28T21:12:52.457000	2022-09-28T21:52:57.457000	2405.199625	NICHOLS
● OEOW17FIQ	JUPITER-AURORA-JUNOEM-17	2022-10-01T19:02:08.457000	2022-10-01T19:42:13.457000	2405.199875	NICHOLS
OEZ020M2Q	JUPITER-AURORA-JUNOEM-20	2022-11-05T23:18:13.540000	2022-11-06T00:01:07.540000	2574.199875	NICHOLS
● OEZ019QRQ	JUPITER-AURORA-JUNOEM-19	2022-11-06T05:39:04.547000	2022-11-06T06:21:58.547000	2574.2	NICHOLS
OEZ021AKQ	JUPITER-AURORA-JUNOEM-21	2022-11-07T00:41:35.557000	2022-11-07T01:23:38.557000	2523.2	NICHOLS
● OEZ023XAQ	JUPITER-AURORA-JUNOEM-23	2022-12-15T02:44:28.630000	2022-12-15T03:20:31.630000	2163.2	NICHOLS
OEZ024XKQ	JUPITER-AURORA-JUNOEM-24	2022-12-15T05:54:53.620000	2022-12-15T06:30:56.620000	2163.2	NICHOLS

- Data in which the Europa footprint was detected.

A4. HST/STIS data analysis: the lead angle

We used an *Astropy* module *photutils* to locate the Europa footprint and measure the brightness.

Locating the footprints

- *DAOStarFinder* searches and lists bright spots with a given radius in a fits image.
- Europa's MAW spot is manually (by eye) chosen out of the list based on JRM33+CON20 model predicts of:
 - Europa's instantaneous footprint and
 - The reference line of Europa's footprint.

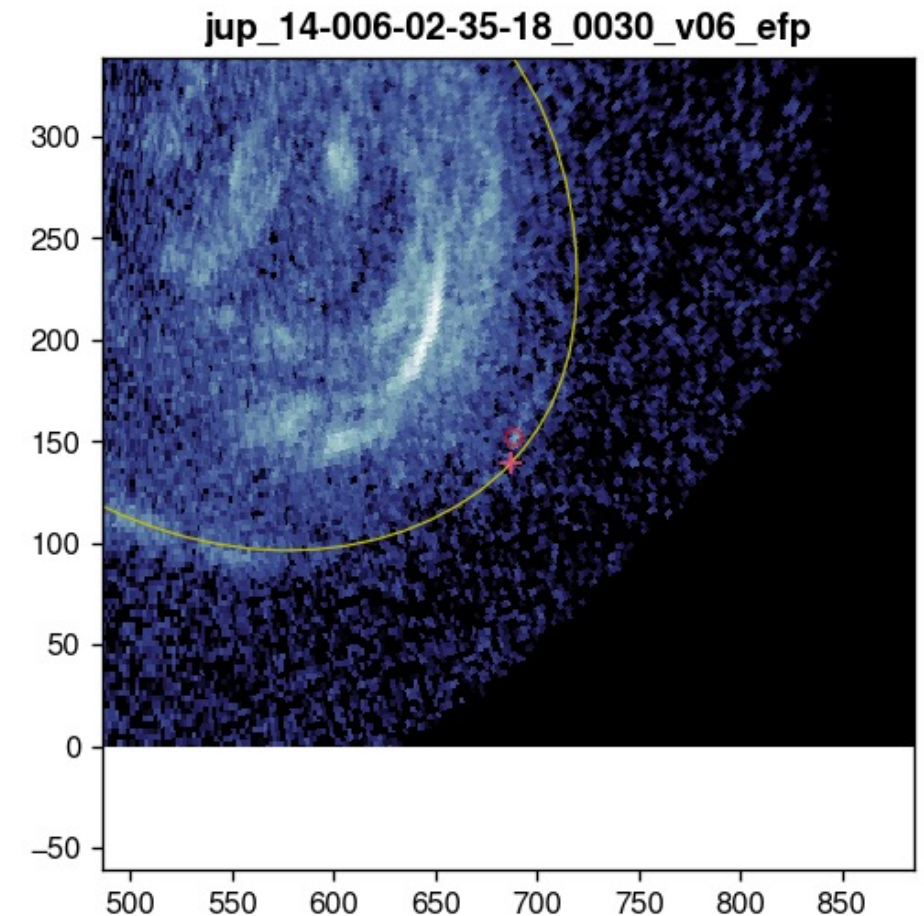


Fig A0401. An example of the polar-projected image of Jupiter's northern hemisphere. The red circle shows Europa's MAW spot.

A4. HST/STIS data analysis: the lead angle

Errors of footprint location

- Accuracy of footprint location depends on:
 - Offsets from the actual sub-observer point as Jupiter's disk images are extracted in the polar coordinate and
 - Errors in manually choosing the spot out of the list of *DAOStarFinder*.
- We calculated the total spatial errors in longitude and latitude for each HST visit.

Table A0401. Spatial errors of the observations.

CML	± 0.15 deg
Locating the spot	± 0.34 deg

A5. HST/STIS data analysis: the brightness

- Measurement (photometry) of the footprint brightness is done by *aperture_photometry* of *photutils*.
- Measurement of brightness of the MAW spot requires:
 - Separation of the MAW spot and the tail structure and
 - Measurement of the background brightness.

We measure background brightness in a region defined with half of a ring in order to exclude the tail brightness.

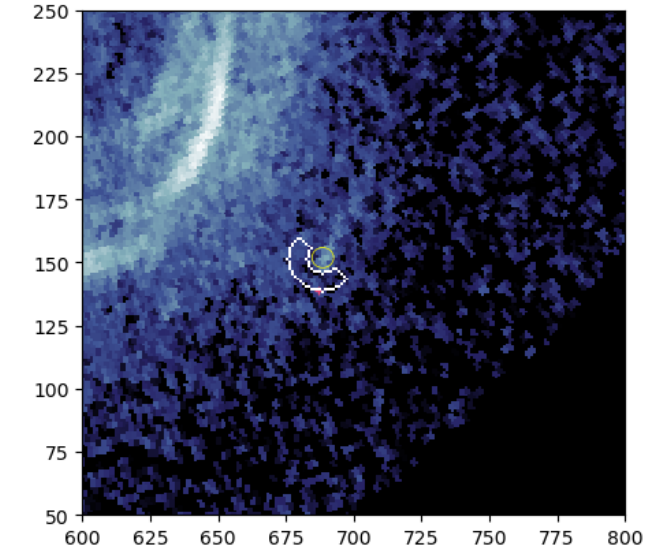
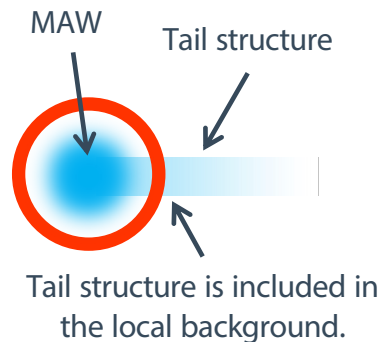
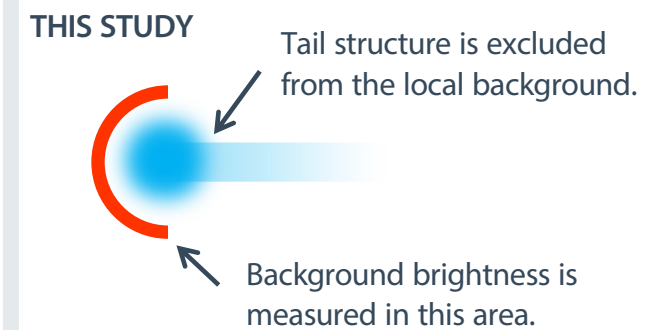


Fig A0501. Boundary of the area that defines a local background brightness.



A6. Magnetic field model

Jupiter's magnetic field

- JRM33 Jupiter's magnetic field model (Connerney+2022):
 - Represented with a degree 30 spherical harmonic.
 - Coefficients were determined by the magnetic field observations acquired by the Juno spacecraft during 32 of its first 33 polar orbits.
 - P_n^m are Schmidt quasi-normalized associated Legendre functions of degree n and order m .

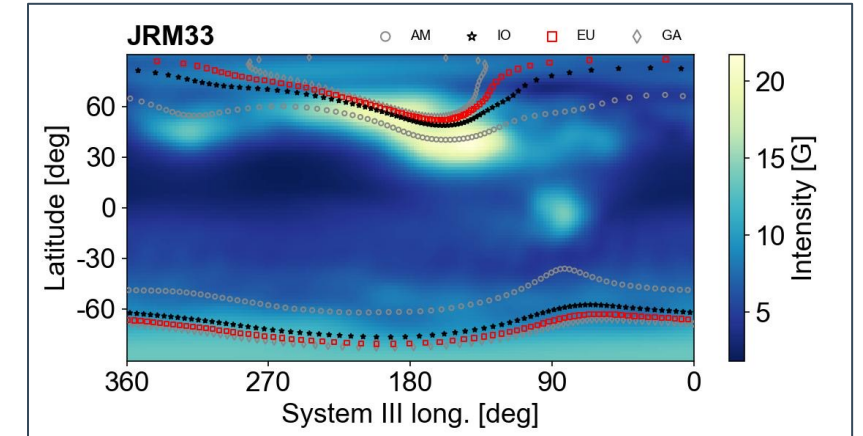


Fig A0601. Magnetic field strength on Jupiter's surface (1/15.4 dynamically flattened) calculated by JRM33 model (Connerney+2021). The scatter plots show the location of the satellite footprint of Amalthea, Io, Europa, and Ganymede.

$$\vec{B} = -\nabla V_p + \vec{b} \quad v_p = a \sum_{n=1}^{n_{\max}} \left(\frac{a}{r}\right)^{n+1} \sum_{m=0}^n \{ P_n^m(\cos \theta) [g_n^m \cos(m\phi) + h_n^m \sin(m\phi)] \}$$

A6. Magnetic field model

Jupiter's magnetic field

- Current sheet model (Connerney+2020):
 - Simple empirical magnetodisc model that describes the magnetic field in the inner and middle magnetosphere of Jupiter.
 - Best fit parameters are given based on the observations at Juno's first 24 orbits.

Table 1
Magnetodisc Parameters

Parameter	Value	Description	Units
R_0	7.8	Disc inner radius	Jovian radii
R_1	51.4	Disc outer radius	Jovian radii
D	3.6	Half thickness	Jovian radii
$\mu_0 I/2$	139.6	Current constant	nT
θ_D	9.3	Disc normal from rotation axis	degrees
φ_D	204.2	Azimuth angle of disc normal	degrees

$$B_\rho = \left(\frac{\mu_0 I_0}{2} \right) \frac{\rho}{2} \left(\frac{1}{F_1} - \frac{1}{F_2} \right) \quad B_\phi = 0$$

$$B_z = \left(\frac{\mu_0 I_0}{2} \right) \left(\frac{2D}{\sqrt{z^2 + a^2}} - \frac{\rho^2}{4} \left(\frac{z-D}{F_1^3} - \frac{z+D}{F_2^3} \right) - \frac{2D}{\sqrt{z^2 + b^2}} \right)$$

$$F_1 = \sqrt{(z-D)^2 + a^2} \quad F_2 = \sqrt{(z+D)^2 + a^2}$$

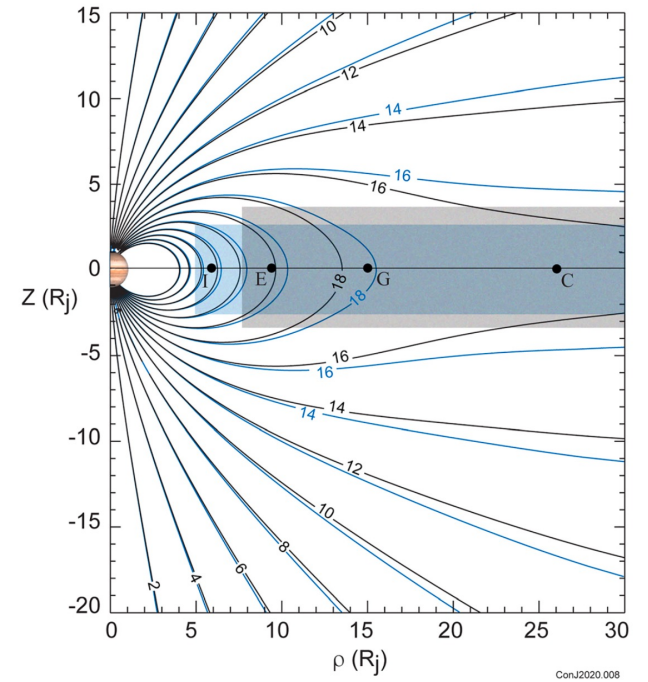


Fig A0602. Schematic illustration of the current sheet model by Connerney+2020.

A7. Evaluation of the fitting

- Parameters:
 - Plasma (ion) mass density ρ_0 [amu cm⁻³]
 - Ion core temperature T_i [K] → Vertical scale height of the plasma sheet
- Confidence limits on fitted parameters (ρ_0 and T_i) are estimated based on the chi-square value χ^2 .
- Contour lines of constant $\Delta\chi^2$ are drawn in the two-dimensional parameter space to show the confidence limits.

$$H = \sqrt{\frac{2k_B T_i}{3m_p A_i \Omega^2}}$$

Bagenal & Delamere (2011)

Table A0701. Chi-square confident level for p-values.

p-value	$\Delta\chi^2$
68.3% (1 σ)	2.30
90%	4.61
95.4% (2 σ)	6.17
99%	9.21
99.73% (3 σ)	11.8
99.99%	18.4

A7. Evaluation of the fitting

- The chi-square value χ^2 is defined as follows:

$$\chi^2 = \sum_{i=1}^N \left(\frac{y_i - y(x_i; a_1, a_2)}{\sigma_i} \right)^2$$

N : number of data points

a_1, a_2 : adjustable parameters of the model function y $\longrightarrow \rho_0$ and T_i

x_i, y_i : the data set $\longrightarrow x_i$ = Europa's System III longitude

y : model function $\longrightarrow y_i$ & y = Equatorial lead angle

σ_i : standard deviation of data point y_i \longrightarrow Errors in location of the footprints

- Difference ($\Delta\chi^2$) between each χ^2 and the minimum value χ^2_{\min} out of the entire model estimations.

$$\Delta\chi^2(\mathbf{a}) = \chi^2(\mathbf{a}) - \chi^2_{\min}$$

a : vector of adjustable parameters $\longrightarrow \rho_0$ and T_i

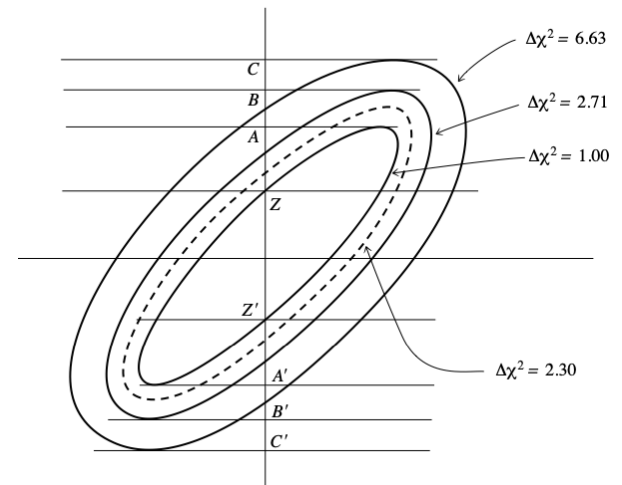


Fig A0701. Confidence region ellipses corresponding to values of chi-square larger than the fitted minimum (*Numerical recipe in C*).

Appendix

A7. Evaluation of the fitting

- We calculate $\Delta\chi^2$ to evaluate fit of the two parameters.
- The best-fit parameter set is derived as follows:

Table A0702. Chi-square minima of the fitting for 2014 and 2022 data.

Day of year	6, 13, 16 (in 2014)	271, 274 (in 2022)
ρ_0 [amu cm $^{-3}$]	1703	2746
T_i [eV]	72	138
χ^2_{\min}	14.719	2.256

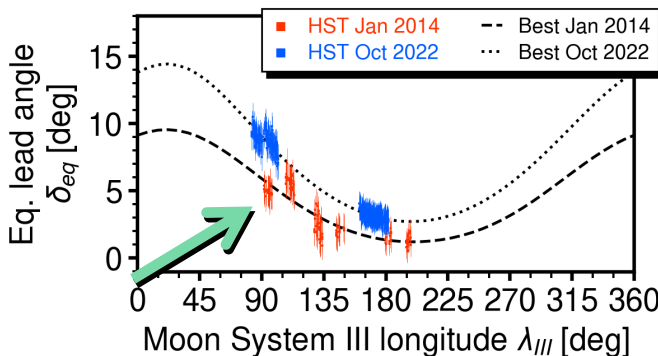


Fig A0702. Fitting curves and the HST observations.

Fluctuation at $\lambda_{\text{III}} \sim 90^\circ$ in 2014
is not replicated by our model.
→ Larger χ^2_{\min} in 2014.

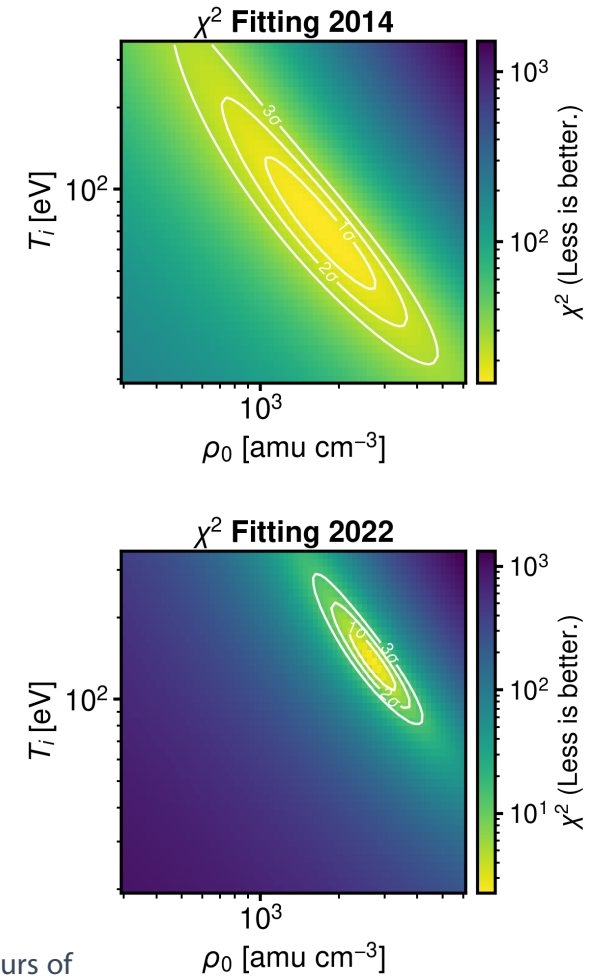


Fig A0703. Contours of the fitting confidence level.